expansion about the local-oscillator voltage v_j:

$$i_g(v) = i_g(v_j) + \frac{di_g}{dv}\bigg|_{v_j} (v - v_j) + \cdots \qquad \text{(A-1a)}$$

$$Q(v) = Q(v_j) + \frac{dQ}{dv}\bigg|_{v_j} (v - v_j) + \cdots \qquad \text{(A-1b)}$$

where

$$\frac{di_g}{dv}\bigg|_{v_j} \equiv G(v_j) = \text{differential junction conductance} \qquad \text{(A-2a)}$$

$$\frac{dQ}{dv}\bigg|_{v_j} \equiv C(v_j) = \text{differential junction capacitance.} \qquad \text{(A-2b)}$$

The total current i through the junction due to the applied local-oscillator voltage is given by

$$i = i_g(v_j) + \dot{Q}(v_j)$$

where

$$i_g(v_j) = I_s[\exp(\alpha v_j) - 1]$$

and[1]

$$\dot{Q}(v_j) = C(v_j)\frac{dv_j}{dt}.$$

Thus

$$i = I_s[\exp(\alpha v_j) - 1] + C(v_j)\frac{dv_j}{dt}. \qquad \text{(A-3)}$$

ACKNOWLEDGMENT

The authors wish to thank Miss M. L. Hadley for invaluable assistance in computer programming, M. J. Urban for providing the GaAs Schottky-barrier diode, V. A. Lanzisera for performing the measurements, and Dr. B. A. Shortt for helpful advice and direction.

[1] Note that $Q(v_j)$ does not equal $d/dt[C(v_j)v_j]$ since $C(v_j)$ is the differential capacitance. Thus $\dot{Q}(v_j) = (dQ(v_j)/dv_j)(dv_j/dt)$ where $(dQ(v_j)/dv_j) \equiv C(v_j)$. See [12].

REFERENCES

[1] H. C. Torrey and C. A. Whitmer, *Crystal Rectifiers* (M.I.T. Radiation Laboratory Series), vol. 15. New York: McGraw-Hill, 1948.
[2] P. D. Strum, "Some aspects of mixer crystal performance," *Proc. IRE*, vol. 41, pp. 875–889, July 1953.
[3] G. C. Messenger and C. T. McCoy, "Theory and operation of crystal diodes as mixers," *Proc. IRE*, vol. 45, pp. 1269–1283, Sept. 1957.
[4] C. F. Edwards, "Frequency conversion by means of a nonlinear admittance," *Bell Syst. Tech. J.*, vol. 35, p. 1403, 1956.
[5] A. C. Macpherson, "An analysis of the diode mixer consisting of nonlinear capacitance and conductance and ohmic spreading resistance," *IRE Trans. Microwave Theory Tech.*, vol. MTT-5, pp. 43–51, Jan. 1957.
[6] C. A. Liechti, "Down-converters using Schottky-barrier diodes," *IEEE Trans. Electron Devices*, vol. ED-17, pp. 975–983, Nov. 1970.
[7] M. R. Barber, "Noise figure and conversion loss of the Schottky-barrier mixer diode," *IEEE Trans. Microwave Theory Tech.*, vol. MTT-15, pp. 629–635, Nov. 1967.
[8] L. D. Cohen, "Microwave characterization of the properties and performance of GaAs Schottky barrier mixer diodes," *Proc. IEEE* (*Special Issue on Satellite Communications*) (Lett.), vol. 59, pp. 288–289, Feb. 1971.
[9] G. A. Korn and T. M. Korn, *Mathematical Handbook for Scientists and Engineers*. New York: McGraw-Hill, 1968.
[10] M. Abromowitz and I. A. Stegun, *Handbook of Mathematical Functions* (Applied Mathematics Series 55). Washington, D. C.: NBS, 1967.
[11] Microwave Associates, Inc., "High rf burnout resistance mixer diodes," *Microwave J.*, vol. 13, p. 26, 1970.
[12] L. Blackwell and K. Kotzebue, *Semiconductor-Diode Parametric Amplifiers*. Englewood Cliffs, N. J.: Prentice-Hall, 1961, p. 107.

Design of Evanescent-Mode Waveguide Diplexers

C. K. MOK

***Abstract*—A novel design procedure for diplexers built in waveguides below cutoff is presented. The design permits the integral construction of a diplexer—the whole unit is built in a single waveguide, thereby dispensing with the T junction and connecting flanges—if coaxial termination is used at the common junction. The design utilizes foreshortened bandpass filters, and is valid for bandwidths of up to a few percent. Simple expressions on calculating the connecting lengths are arrived at. A satellite telemetry diplexer designed using the derived expressions yields results which are in agreement with computed values.**

Manuscript received May 1, 1972; revised July 21, 1972. This project was sponsored by the European Space Research Organisation.

The author is with the Standard Telecommunications Laboratories, an Associate of International Telephone and Telegraph, London Road, Harlow, Essex, England.

I. INTRODUCTION

DIPLEXERS in general take the form of two filters connected to a common port, and a fundamental problem in a diplexer is the matching of the two filters into this port. Various methods of diplexer design have been described in the past. Among these is the use of singly terminated low-pass and high-pass filters with Butterworth characteristics, which may be designed to be fully complementary [1], and hence may be connected together without the need of a correction network. This complementary nature is not present in Chebyshev singly terminated filters, and Veltrop and Wilds [2] have derived tables for quasi-complementary diplexers. Matthaei and Cristal [3] have described a design of partly complementary diplexers using foreshortened low-pass and bandpass doubly terminated Chebyshev filters typically with an odd number of sections; the residual susceptance is tuned out by an annulling network. The last approach is the one adopted here, mainly because, in the evanescent-mode medium, the annulling network is already partially present.

The general principles and applications of evanescent-mode waveguides have been described in various publications [4]–[6]. The design theory of diplexers in this medium is a natural extension to the design of such filters, described elsewhere [7]. With coaxial termination at the common port, the theory permits the construction of the diplexer in a single waveguide body. This obviates the need for the conventional T junction and connecting flanges, thereby providing substantial reduction in weight and bulk.

The design here uses bandpass filters and is valid for bandwidths of up to a few percent. Additional channels may be dropped in the manner suggested by Wenzel [1], i.e., by cascading.

II. Evanescent-Mode Filter Design

A few explanatory notes on evanescent-mode filter design are in order. The two basic building blocks of an evanescent-mode filter are a length of below cutoff waveguide (forming the coupling and the inductance of the resonator) and a capacitive obstacle (tuning screw, dielectric, etc.). In circuit terms, a section of evanescent-mode waveguide of length l_r may be characterized by a J-inverter shunted at each end by an inductance, Fig. 1(a) and (b). In the figures, each impedance has been normalized to the characteristic impedance of the waveguide. In the present application of uniform waveguide size the definition of the guide impedance is unimportant. Where a change in guide occurs, as when the two outer ports are to be matched to propagating waveguides, [7] gives the appropriate equations. With coaxial termination, the evanescent-mode medium differs from that of the conventional propagating waveguide. In the latter, the customary practice is to design so that the input impedance (looking into the waveguide port) of the transition equals the characteristic (real) impedance of the waveguide; in the former, the absence of a real characteristic impedance means that there is not a natural preferred operating impedance. Thus the coaxial probe may be located at the plane of a capacitive post (region of high electric field), and hence should present a high impedance for match, or it may be positioned some distance away where a lower impedance is needed. Currently, the design of such transitions is empirical but not at all difficult.

The normalized admittance parameter J_r and the phase shift ϕ of the inverter in Fig. 1 are, respectively:

$$J_r = \frac{1}{\sinh \gamma l_r} \tag{1a}$$

$$\phi = \frac{\pi}{2} \text{ at all frequencies} \tag{1b}$$

while the shunting inductive susceptance B_{sr} at each end is

$$B_{sr} = \coth \gamma l_r. \tag{1c}$$

The equivalent circuit of a multisection filter may be drawn as

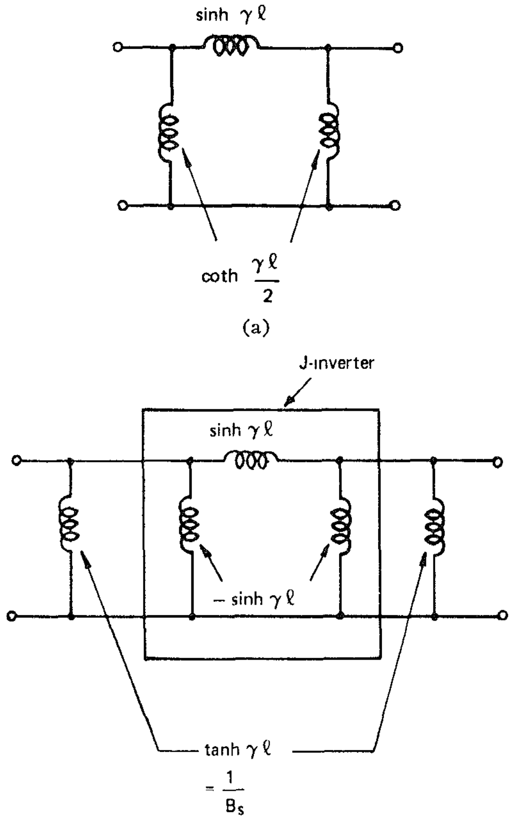

(b)

Fig. 1. (a) Equivalent circuit of length of evanescent-mode waveguide, showing normalized impedances. (b) Equivalent circuit redrawn with J-inverter, showing normalized impedances.

in Fig. 2 where B_{so} and B_{sn} are the input admittances of short-circuited waveguides to close the filter, assuming that coaxial terminations are used. The value of G is obtained by equating the first cavity loaded Q of the evanescent-mode filter to that of the suitably transformed bandpass lumped circuit filter and is

$$G = \frac{1}{\Delta \frac{f}{b} g_1 \frac{1}{\coth \gamma l_0 + \coth \gamma l_1}} \tag{2a}$$

$$\simeq \frac{2}{\Delta \frac{f}{b} g_1} \qquad \text{for narrow bandwidths} \tag{2b}$$

where

$$\Delta = \frac{2}{1 + \frac{1}{1 - (f/f_c)^2}}$$

a correction factor to account for the steeper slope of the evanescent-mode "inductance."

f frequency,
f_c cutoff frequency,
b 3 dB or equal-ripple bandwidth.

The lengths between the tuning screws may be obtained from

$$\sinh \gamma l_r = \Delta \frac{f}{b} \sqrt{g_r \cdot g_{r+1} \frac{1}{\coth \gamma l_{r-1} + \coth \gamma l_r} \cdot \frac{1}{\coth \gamma l_r + \coth \gamma l_{r+1}}} \tag{3a}$$

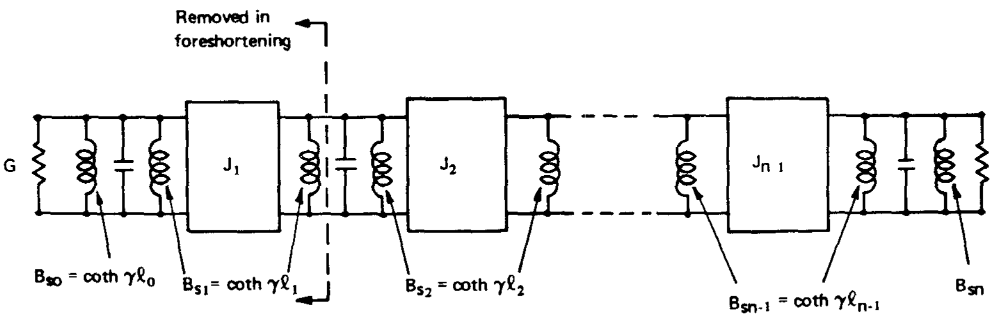

Fig. 2. Equivalent circuit of evanescent-mode filter with J-inverters, normalized admittances.

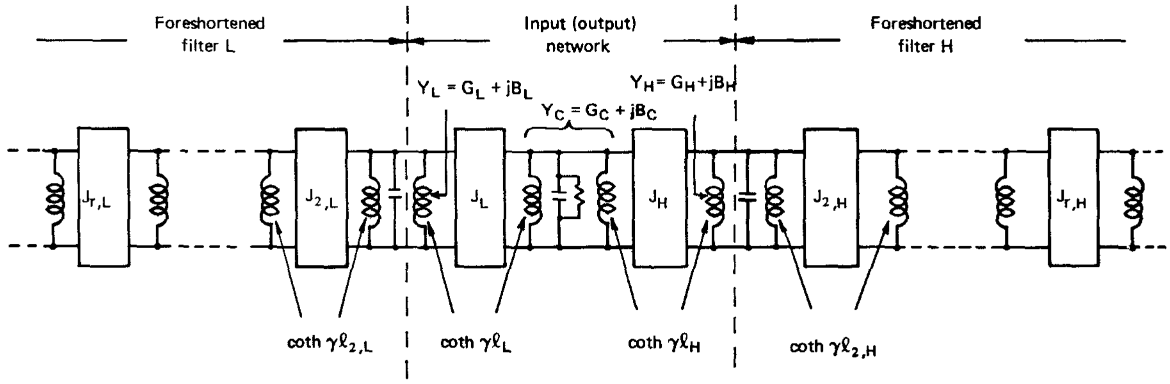

Fig. 3. Equivalent circuit of diplexer.

$$\cong \frac{1}{2}\Delta\frac{f}{b}\sqrt{g_r g_{r+1}} \qquad \text{for narrow bandwidths} \tag{3b}$$

where

l_r length between rth and $(r+1)$th screws,

g_r rth element of low-pass prototype filter (see Fig. 4).

III. Diplexer Design

The approach here, based on the work of Matthaei and Cristal [3], utilizes foreshortened filters, i.e., filters with the first element removed (see Fig. 2) to obtain a partly complementary pair of filters; the residual susceptance at each center frequency is then tuned out by an annulling network at the common port. The circuit of such an arrangement in cutoff waveguide is in Fig. 3. The annulling network is shown as B_c, whose inductive branch is derived from the evanescent-mode waveguide; introducing the capacitive post at this plane completes the annulling circuit. The problem is to determine the connecting lengths l_L and l_H.

At the center frequency of filter L, i.e., at f_L, Y_L is real and equals G_L, while Y_H is imaginary and equals jB_H. Therefore, the combined admittance of the two filters at the center plane is

$$Y_{t(L+H)} = \frac{J_L^2}{G_L} + \frac{J_H^2}{jB_H}$$

$$= \frac{1}{G_L \sinh^2 \gamma l_L} + \frac{1}{jB_H \sinh^2 \gamma l_H}. \tag{4a}$$

Likewise at f_H,

$$Y_{t(L+H)} = \frac{1}{G_H \sinh^2 \gamma l_H} + \frac{1}{jB_L \sinh^2 \gamma l_L}. \tag{4b}$$

The conditions for match are clearly

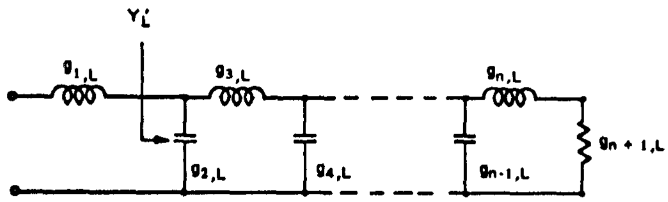

Fig. 4. Low-pass prototype of filter L.

$$G_c = \frac{1}{G_L \sinh^2 \gamma l_L} = \frac{1}{G_H \sinh^2 \gamma l_H} \tag{5}$$

and

$$B_c = \frac{1}{B_H \sinh^2 \gamma l_H}, \qquad \text{at } f_L \tag{6a}$$

$$B_c = \frac{1}{B_L \sinh^2 \gamma l_L}, \qquad \text{at } f_H \tag{6b}$$

from which

$$\sinh \gamma l_H = \sqrt{\frac{1}{B_c B_H}} \tag{7a}$$

and

$$\sinh \gamma l_L = \sqrt{\frac{1}{B_c B_L}}. \tag{7b}$$

The quantities B_L, B_H, and B_c are as yet unknown and have to be determined. For the susceptances B_L and B_H, use is made of the low-pass prototype filters. Thus for B_L, the input admittance of the foreshortened prototype filter Y_L' is given by (see Fig. 4)

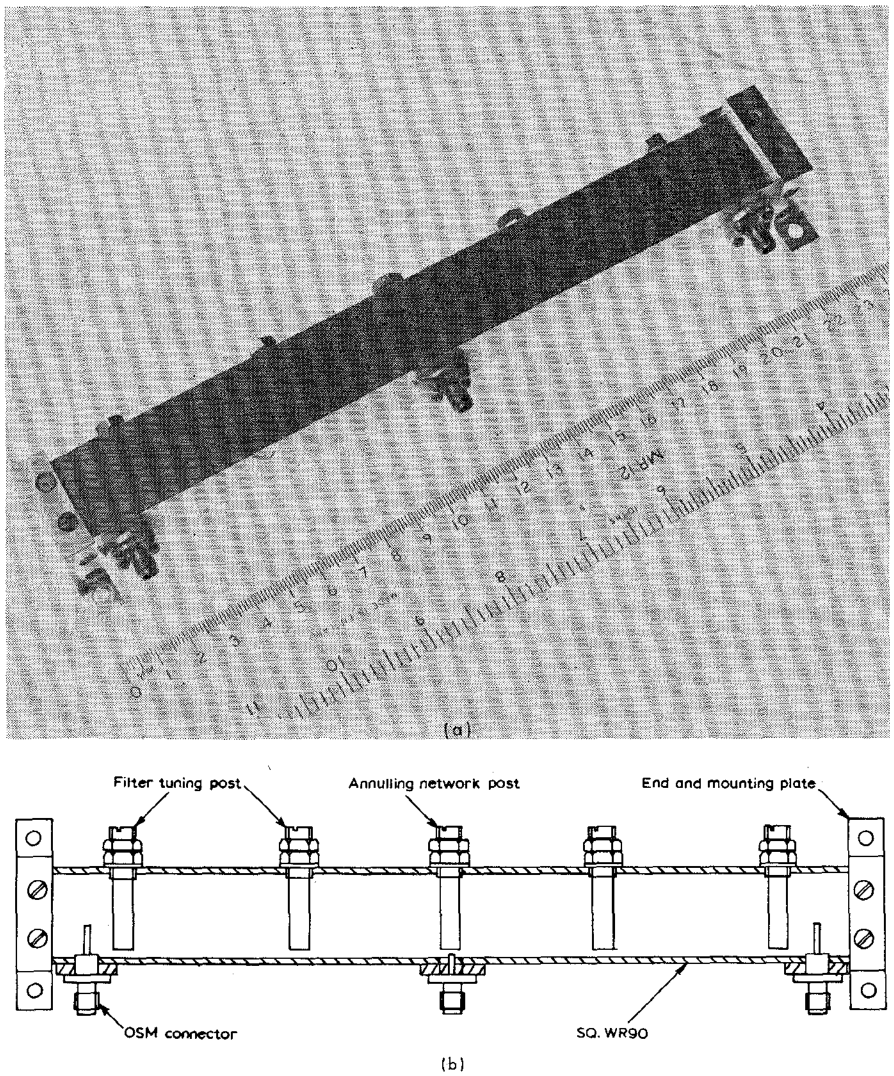

Fig. 5. (a) S-band telemetry diplexer. (b) Drawing of S-band telemetry diplexer, showing details.

$$Y_L' = G_L' + jB_L' = j\omega' g_{2,L} + \cfrac{1}{j\omega' g_{3,L} + \cfrac{1}{j\omega' g_{4,L} + \cfrac{1}{\ddots}}} + \cfrac{1}{j\omega' g_{n,L} + \cfrac{1}{g_{n+1,L}}} \tag{8}$$

from which B_L' may be extracted. It is required to determine the value of B_L at f_H so that in the above equation

$$\omega' = \frac{f_H - f_L}{\frac{1}{2} b_L}. \tag{9}$$

Having obtained B_L' the value of B_L follows, from

$$B_L = B_L' \times G_L \tag{10}$$

with G_L given by, from (2)

$$G_L \simeq \frac{2}{\Delta \dfrac{f_L}{b_L} g_{2,L}}. \tag{11}$$

Similar expressions hold for B_H and G_H; B_H is of opposite sign to B_L.

Looking at Fig. 3, it is seen that the inductive branch of B_c is $(\coth \gamma l_L + \coth \gamma l_H)$. If the resonant frequency of B_c is at f_0, then at a frequency deviation of $\pm \delta f$ from f_0, B_c is given by

$$B_c = 2(\coth \gamma l_L + \coth \gamma l_H) \frac{\delta f}{\Delta f_0}, \qquad f_0 \gg \delta f \tag{12a}$$

which may be approximated to

$$B_c \simeq 4 \frac{\delta f}{\Delta f_0} \qquad \text{for narrow bandwidths.} \tag{12b}$$

The position of f_0 in relation to f_L and f_H, or $\delta f_L (= f_L - f_0)$ and $\delta f_H (= f_H - f_0)$, is easily obtained from (6) and (12); thus

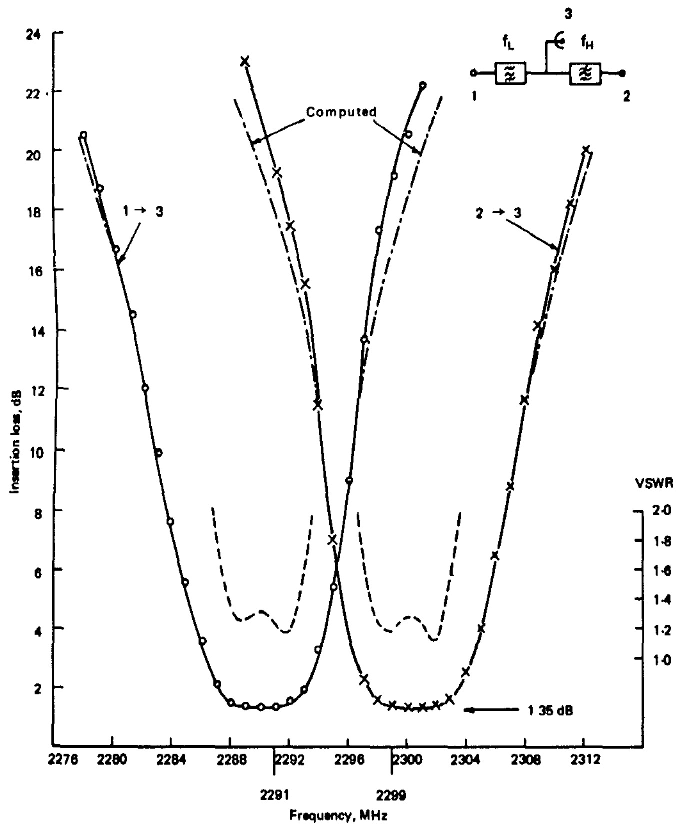

Fig. 6. Measured transmission response.

at f_L

$$4\left|\frac{\delta f_L}{\Delta\cdot f_0}\right| = \left|\frac{1}{B_H \sinh^2 \gamma l_H}\right| = \left|\frac{1}{B_H' G_H \sinh^2 \gamma l_H}\right|. \tag{13a}$$

Likewise, at f_H

$$4\left|\frac{\delta f_H}{\Delta\cdot f_0}\right| = \left|\frac{1}{B_L' G_L \sinh^2 \gamma l_L}\right|. \tag{13b}$$

Dividing (13a) by (13b),

$$\left|\frac{\delta f_L}{\delta f_H}\right| = \left|\frac{B_L' G_L \sinh^2 \gamma l_L}{B_H' G_H \sinh^2 \gamma l_H}\right| = \left|\frac{B_L'}{B_H'}\right| \text{ from (5).} \tag{14}$$

Equation (14) thus defines the position of f_0 with respect to f_L and f_H, in terms of the low-pass prototype susceptances.

The two lengths l_L and l_H may now be calculated, thus substituting (10) and (12b) into (7) we finally have

$$\sinh \gamma l_H \simeq \frac{1}{2}\sqrt{\Delta \frac{f_0}{\delta f_L}\cdot\frac{1}{B_H' G_H}} \tag{15a}$$

$$\sinh \gamma l_L \simeq \frac{1}{2}\sqrt{\Delta \frac{f_0}{\delta f_H}\cdot\frac{1}{B_L' G_L}}\,. \tag{15b}$$

To summarize the design procedure:

1) design each foreshortened filter to begin with a shunt resonator, using (3),
2) determine G_L (and G_H) from (11),
3) determine B_L' (and B_H') from (8),
4) determine δf_L, δf_H, and hence f_0, from (14),
5) determine $\sinh \gamma l_L$ and $\sinh \gamma l_H$ from (15), and hence l_L and l_H.

IV. Experimental Results

Following the procedure outlined, a telemetry diplexer, consisting of a pair of foreshortened 3-section filters with 0.01-dB passband ripple was designed. The filter bandwidths are 4.72 MHz, with center frequencies at 2290 MHz and 2300 MHz.

The diplexer, shown in Fig. 5(a) and (b), was designed for satellite application, and therefore was constructed in aluminum waveguide (square WR90). A technique for temperature compensation exists which permits construction in the light-weight material, and temperature stability is achieved without recourse to the heavier Invar waveguide. With the aluminum construction and the absence of connecting flanges and T junction an overall weight of only 170 g is realized.

Measured transmission response and VSWR of each path are depicted in Fig. 6; also depicted in Fig. 6 are the computed transmission responses, which agree well with the measured results. Midband loss per path is 1.37 dB, while VSWR is in the region of 1.25; this slightly high VSWR figure is the result of an intentional decoupling at each input port, to raise the isolation.

In this example design, where the diplexer is required for telemetry, the crossover region is relatively unimportant and the responses cross at about 6 dB, with accompanying poor VSWR. Where maximum usage of bandwidth is essential, as in communication channels, more filter sections are necessary, with crossover designed at 2–3 dB. Under such situations the annulling network is adequate in providing acceptable VSWR figures.

The principal advantage of these filters lies in the large range of volume/loss tradeoff obtainable, permitting losses comparable with conventional waveguide, when larger dimensions may be tolerated. In this particular application, however, the evanescent-mode filter offers no loss advantage over a comparable volume TEM filter, but does have a substantial weight advantage, a prime consideration in satellites. This advantage derives from its use of lightweight material and from the simplicity of the annulling network, part of which (the inductive element) is intrinsic to the structure.

V. Spurious Passbands

These occur above the cutoff frequency of the waveguide. In the above diplexer the first parasitic passband occurs at around 7.3 GHz, which is more than $3f_0$. If necessary, this figure may be improved through the use of smaller size waveguides to 4–$5f_0$ at the expense of loss. Indeed simple broadband ($\sim$30 percent bandwidth) evanescent-mode filters with 3 or 4 cavities, built in guides way below cutoff have been used effectively to replace the much more expensive waffle-iron filters for spurious suppression in low power applications [8].

VI. Conclusion

A design procedure for diplexers with no guard band, in waveguides below cutoff, has been described. Based on this a diplexer has been constructed and tested, yielding results that are in agreement with computed values. The design is valid for bandwidths of up to a few percent and, as it stands, is specifically for coaxial termination at the common port; however, it can be extended to include other terminations at this port. The integral construction of the diplexer, besides its simplicity, results in additional saving in weight in an already lightweight medium. Further size and weight reductions may be obtained through the use of inductive loading [9], with little sacrifice in loss. The small size, light weight, low-loss, and good temperature stability of these units should make them highly attractive in aerospace applications.

Acknowledgment

The author wishes to thank G. Craven for reading the manuscript and for useful comments, and Standard Telecommunication Laboratories Ltd. for permission to publish the paper.

References

[1] R. J. Wenzel, "Application of exact synthesis methods to multichannel filter design," *IEEE Trans. Microwave Theory Tech.* (*1964 Symposium Issue*), vol. MTT-13, pp. 5–15, Jan. 1965.
[2] R. G. Veltrop and R. B. Wilds, "Modified tables for the design of optimum diplexers," *Microwave J.*, vol. 7, no. 6, pp. 76–80, June 1964.
[3] G. L. Matthaei and E. G. Cristal, "Theory and design of diplexers and multiplexers," in *Advances in Microwaves*, vol. 2. New York: Academic Press, 1967, pp. 237–326.
[4] G. Craven and C. K. Mok, "Lightweight microwave components for communication satellites" presented at the Symp. Long Term Prospects for Communication Satellites, Genoa, Italy, June 1971.
[5] G. Craven, "Waveguide below cut-off: A new type of microwave integrated circuit," *Microwave J.*, vol. 13, pp. 51–58, Aug. 1970.
[6] G. A. Hockham, "Flush mounted aeronautical antenna," presented at the IEE Conf. Aerospace Antennas; also in *Conf. Pub. No. 77*, June 1971, pp. 49–53.
[7] G. F. Craven and C. K. Mok, "The design of evanescent mode waveguide bandpass filters for a prescribed insertion loss characteristic," *IEEE Trans. Microwave Theory Tech.*, vol. MTT-19, pp. 295–308, Mar. 1971.
[8] G. Craven, "Slimguide microwave components," *Elec. Commun.*, vol. 47, no. 4, Nov. 1972.
[9] C. K. Mok, D. W. Stopp, and G. Craven, "Susceptance loaded evanescent mode waveguide filters," *Proc. Inst. Elec. Eng.*, vol. 119, no. 4, pp. 416–420, Apr. 1972.

Short Papers

Equivalent Circuit of Reentrant Cavity

KATSUAKI UENAKADA

***Abstract*—In order to develop a design formula for a reentrant cavity, as it changes from the very flat to very long form, the admittance of the cavity at the gap is derived. For the resonant frequency of an air-filled cavity, the theoretical value by the formula derived here agrees well with the experimental value.**

Manuscript received October 12, 1971; revised July 28, 1972.
The author is with the Technical Research Laboratories of Nippon Hoso Kyokai, Tokyo, Japan.

I. Introduction

Reentrant cavities have advantages of simple mechanical construction and wide tuning range, for which they have been used effectively in klystrons. With recent developments in solid-state devices, such as Gunn diodes and varactors, there has been a widespread use of these cavities in the form shown in Fig. 1(a).

In Fig. 1(a), the cylindrical coordinates ρ, ϕ, and Z are used as shown. The radial-line region containing the active solid-state element delineated by $0 \leqq \rho \leqq r_1$, $0 \leqq Z \leqq d$ is designated herein as region A, and the coaxial cavity region bound by $r_2 \geqq \rho \geqq r_1$, $0 \leqq Z \leqq l$, as region B. The admittance Y_a of a cavity having the active solid-state element can be calculated from an analysis of a radial line [5].